DOI: 10.1002/anie.200600060

Microscopic Machines

Chemical Locomotion

*Walter F. Paxton, Shakuntala Sundararajan, Thomas E. Mallouk, and Ayusman Sen**

Keywords:
autonomous motion · heterogeneous catalysis · micromotors · molecular devices · nanotechnology

Research into the autonomous motion of artificial nano- and microscale objects provides basic principles to explore possible applications, such as self-assembly of superstructures, roving sensors, and drug delivery. Although the systems described have unique propulsion mechanisms, motility in each case is made possible by the conversion of locally available chemical energy into mechanical energy. The use of catalysts onboard can afford nondissipative systems that are capable of directed motion. Key to the design of nano- and micromotors is the asymmetric placement of the catalyst: its placement in an environment containing a suitable substrate translates into non-uniform consumption of the substrate and distribution of reaction products, which results in the motility of the object. These same principles are exploited in nature to effect autonomous motion.

1. Introduction

Locomotion in macroscale objects is easily achieved by using engines that consume chemical fuel. Directed motion of micro- and nanoscale objects is desirable for many applications, such as self-assembly of superstructures, roving sensors, drug-delivery systems, and useful nanomachinery. The challenge here is to impart energy to an individual object to bring about its autonomous motion. Once this goal is achieved, more complex tasks for application-oriented nano- and micromotors can be envisioned. Conventional approaches to transport and manipulate matter on the small scale use optical trapping methods to address individual or small groups of objects, and external fields that act on an ensemble of small objects. Biomotors and motile bacteria, on the other hand, are able to propel themselves autonomously, independent of external fields and of one another, by harnessing the chemical potential energy available in their environment to produce directed mechanical forces.[1] Several methods of imparting motion to small objects by using localized physical interactions and chemical reactions have been demonstrated in recent years. This Minireview highlights some of these recent developments and discusses the principles and implications of transducing chemical to mechanical energy on the micrometer scale.

[*] W. F. Paxton, S. Sundararajan, Prof. Dr. T. E. Mallouk, Prof. Dr. A. Sen
Department of Chemistry
The Pennsylvania State University
University Park, PA 16802 (USA)
Fax: (+1) 814-865-1543
E-mail: asen@chem.psu.edu

2. Background

In practice, a variety of external fields have been used for colloidal transport in fluids, such as electrophoresis[2] and magnetophoresis[3] for directing the motion of charged and magnetic particles, respectively. Lesser-known modes such as thermophoresis[4] (migration due to a temperature gradient) and diffusiophoresis[5] (migration due to a concentration gradient) have also been used to achieve colloidal transport. The interactions between these externally applied fields and solid–fluid interfaces were discussed by Anderson.[6] While external fields have been used to sort and separate particles based on their response, this type of transport does not afford the flexibility of moving objects independently. In a fundamentally different alternative, optical tweezers have also been used to manipulate colloidal particles with up to nanometer-scale precision using light gradients.[7] However, optical trapping methods require that particles be moved individually or in small groups.[8]

To achieve independent autonomous motion for objects in a given ensemble would require each entity to generate its own field or motive force. For this to occur, each object must convert chemical energy into mechanical energy. Such an

object is in essence a chemical locomotor; it harnesses the chemical free energy of locally available reagents in its environment and translates it into motion. However, the relevant laws that govern the motion of small-scale objects are, in practice, different from those encountered in macroscopic processes.[9] The motion of micrometer- and submicrometer-sized objects is dominated by viscous rather than inertial forces (i.e., low Reynolds number).[10,11] Consequently, fluid flow profiles on the microscale are laminar rather than turbulent and viscous drag effectively eliminates any momentum-based "coasting" of a micro- or nanoobject in motion. Moreover, a dramatic increase in surface-to-volume ratios for smaller objects favors surface forces, such as those related to interfacial tension, over body forces.[9,12] Another effect that further complicates the motion of small objects suspended in fluids is the effect of molecule–particle collisions arising from thermal diffusion.[13] Because the thermal diffusion of a small object is inversely proportional to its dimensions, to overcome the effects of Brownian motion becomes a significant challenge as the size of the moving object is scaled down.

Research in chemical locomotion and the related scaling effects is important not only for designing application-oriented nano- and micromotors but also for understanding the interfacial phenomena related to colloidal transport. Synthetic motors may also be used as simplified mimics to probe unanswered questions pertaining to locomotion in natural systems. A case in point is the motile *Synechococcous* cyanobacteria found in a marine environment.[14] Unlike most other motile microorganisms they do not have typical motility-imparting appendages like the flagella or cilia, and the basis of propulsion in these marine bacteria is not yet fully understood. Besides cell motility, there are questions relating to mechanisms of chemotaxis in certain microorganisms whose sensitivity makes them difficult to test. Artificial systems could also be used to study this problem as they can be engineered to be more robust than their natural counterparts and may be subjected to harsher conditions.

3. Biomotors

To aid us in designing chemical locomotors, we can take a cue from naturally occurring motors. A few notable examples are the motor proteins: kinesins, myosins, and dyneins.[15] These linear nanoscale motors move along complementary tracks and perform a variety of functions such as cytokinesis, signal transduction, intracellular trafficking, and locomotion of cellular components. These biomotors have mechanisms in place to convert chemical energy into the desired mechanical output. While each of these biomotors performs a different function, they share a few common features: they hydrolyze adenosine triphosphate (ATP), which is available in the local environment, to obtain energy, their motion is cyclic and reversible, and they operate with high efficiencies that are not commonly encountered in artificial systems.

Natural systems exhibit asymmetry in their design which allows the locally available energy to be expended non-uniformly, resulting in directed mechanical forces. This feature of asymmetrical configuration is evident from the motility of the bacteria *Listeria monocytogenes*, a pathogen that propels itself by polymerizing actin in the host cell.[16] The

Walter F. Paxton received an AAS degree from Ricks College in Rexburg (now Brigham Young University (BYU-Idaho)) in 1998 and graduated from BYU with a BS in Chemistry in 2001. His research interests initially involved exploring the copper-based polymerization of acrylates, and he later became interested in catalytic motors and electrokinetic phenomena. He recently received the American Chemical Society Inorganic Chemistry Young Investigator Award in Nanoscience for his work on catalytic nanomotors.

Thomas E. Mallouk completed his PhD at the University of California, Berkeley. Following a postdoctoral stay at MIT, he joined the University of Texas at Austin in 1985. In 1993 he joined Pennsylvania State University, where he is now DuPont Professor of Materials Chemistry and Physics. His research interests have spanned inorganic self-assembly and the chemistry of porous, lamellar, and nanoscale materials. He is Director of the Penn State MRSEC Center for Nanoscale Science.

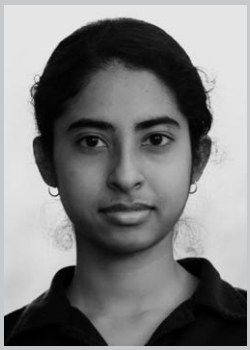

Shakuntala Sundararajan was born in Madras, India. She received her MSc in Chemistry from the Indian Institute of Technology in Madras. She is currently working towards her PhD under the guidance of Prof. Ayusman Sen at Pennsylvania State University. Her research interests include investigations of the mechanism of motility in metallic nanorods and the development of applications thereof.

Ayusman Sen was born in Calcutta, India, and completed his PhD at the University of Chicago, where he was first introduced to catalysis. Following a postdoctoral stay at the California Institute of Technology, he joined Pennsylvania State University, where is currently Head of the Chemistry Department. His honors include an Alfred P. Sloan Fellowship and the Paul J. Flory award from IBM, and he is a Fellow of the American Association for the Advancement of Science. His research interests encompass catalysis, organometallic and polymer chemistry, and nanotechnology.

bacterial protein ActA, which catalyzes the polymerization of actin (a protein found in abundance in eukaryotic cells) into polar filaments, is concentrated on one end—the tail—of the cell. The motility-imparting process occurs in a treadmill fashion: polymerization begins at the tail, while ATP-assisted depolymerization occurs at the other end of the polymer filament. Although the polymerization of actin is believed to play a role in cell deformation and motility in a number of eukaryotic systems, the finding that a single bacterial protein ActA was responsible for motility in *Listeria* provided a simple system to investigate the mechanism.[17] Theriot and co-workers demonstrated that this ActA polymerization enzyme can be used to move nonbiological objects up to 2 μm long (polystyrene beads) by functionalizing them asymmetrically with the ActA polymerization enzyme and releasing them in an actin-rich environment.[18]

The efficiency and the myriad functions carried out by biomotors make them ideal models for artificial nanomotors. However, this versatility is based on an increase in structural complexity. Rather than trying to design artificial biomotors, efforts have been made to transpose these in vivo motors to favorable in vitro conditions. Hybrids of biomotors and nano- or microscale inorganic components have been fabricated, thus illustrating that biomotors can function outside their natural environment. For example, the kinesin–microtubule system has been used outside biological systems to transport inorganic components, such as gold nanowires, over immobilized microtubule tracks.[19,20] This configuration has been inverted to transport microtubule filaments functionalized with magnetic nanoparticles over an array of surface-immobilized kinesins.[21]

Another hybrid system was demonstrated by Montemagno and co-workers in which the enzyme ATPase was used to drive the rotation of submicrometer-sized nickel rods in the presence of ATP fuel solution for a few hours (Figure 1).[22]

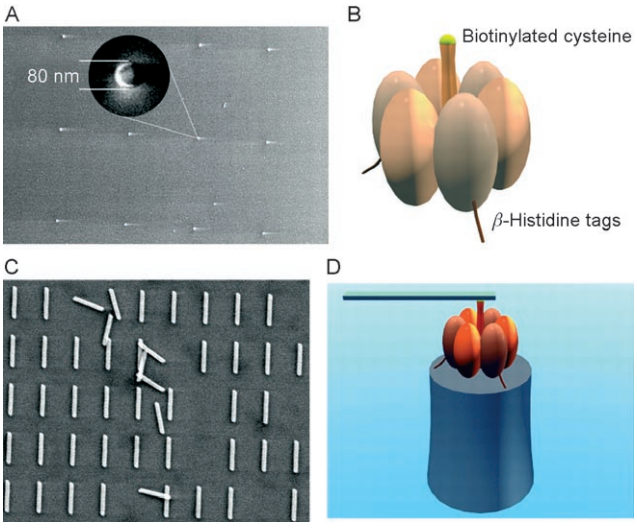

Figure 1. A nanomechanical device (D) powered by an F1-ATPase biomolecular motor and consisting of a Ni post (A; height 200 nm, diameter 80 nm), the F1-ATPase biomolecular motor (B), and a nanopropeller (C; length 750–1400 nm, diameter 150 nm). From Ref. [22].

However, the fraction of functional structures was low as a result of the difficulty in forming ATPase–Ni propeller units that were not pinned down to the underlying substrate. Related approaches have been aimed at fabricating hybrid devices that exploit motile bacteria to drive microscale devices or deliver cargo. Mirkin, Holz, and co-workers demonstrated that surface bound *E. coli* cells exhibit motility and remain live for up to four hours.[23] The feasibility of operating a microbe-powered micromotor based on this method remains to be tested. The precise placement of the bacteria and the prolonged operation of such a device are some of the challenges to this approach. Whitesides and co-workers described another hybrid approach, in which polystyrene beads were attached to photosynthetic unicellular algae (*Chlamydomonas reinhardtii*). They showed that motile microorganisms can be used to move microscale loads.[24]

The problems encountered by Montemagno and others in developing hybrid systems illustrate the intricacies involved in transposing biological motors outside their natural environment, as it is not trivial to mimic in vivo conditions. Even more arduous is replicating biomotors themselves owing to their structural complexity. Besides structural and functional differences, two major themes underlying the operation of biomotors are asymmetry in design and the ability to exploit the supply of locally available high-energy molecules for the transduction of chemical to mechanical energy. Incorporating these ideas of asymmetry and exploiting chemical energy from the environment are keys to the development of autonomously operating synthetic motors.

4. Dissipative Systems

There are a few examples of autonomous motion in chemical systems. The systems discussed in this section involve the lowering of surface free energy due to the interaction between a mobile object and its surrounding medium. A notable example is the selective migration of tin islands on a copper surface.[25] Upon studying the surface alloying of copper–tin at high vacuum, the authors noted that the tin, soon after evaporation on a copper(111) surface, formed islands. Real-time tracking of these tin islands (0.6-μm diameter) using low-energy electron microscopy (LEEM) showed that they migrate selectively over unalloyed copper surfaces to leave behind static bronze features (Figure 2). This selectivity was attributed to the repulsive interaction between moving tin islands and static bronze incorporated on the copper surface.

Another example is that of the spontaneous motion of asymmetric mercury drops when placed in a solution of potassium dichromate and nitric acid.[26] The combination of reactants forms a mercurous chromate product that lowers the surface tension of the reacting mercury surface. Subsequent contact with nitric acid cleanses the surface and exposes fresh mercury for reaction with dichromate. Once set into motion by some spontaneous perturbation of the system, the front of the crescent-shaped drop is constantly exposed to fresh solution while the rear is surrounded by a product-rich environment, thereby maintaining the difference in surface

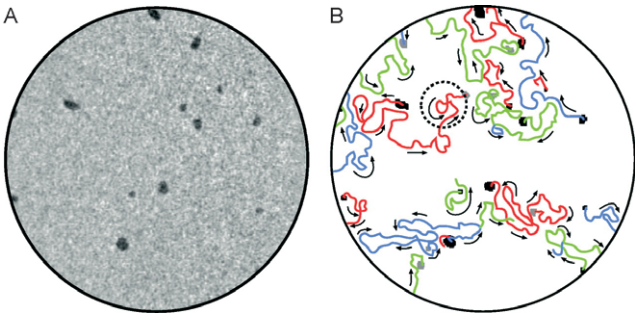

Figure 2. LEEM images (1.5-mm across) of mobile 2D islands on Cu(111). A) Sn islands (dark) formed during Sn deposition on a clean Cu(111) surface (bright background) at 290 K. B) Trajectory plot of migrating Sn islands, demonstrating their tendency to avoid crossing paths. From Ref. [25].

tension between the leading and trailing sides of the moving mercury drop.

Physical processes such as dissolution have also been used to bring about autonomous motion. The motion of camphor solids on a water surface is a well-known example. The dissolution of a scraping of camphor lowers the surface tension of the air–water interface, causing the dissolving "camphor boat" to be propelled over the water surface. An increasing complexity in motion (clockwise, anticlockwise, and unidirectional) has been demonstrated by changing the shape of the piece of camphor.[27] Amphiphilic polymer gels such as poly(*n*-stearyl acrylate) behaved in a similar fashion when they were swollen in tetrahydrofuran and placed on a water surface.[28] As with the case of the dissolving camphor, the swelling solvent has a lower surface tension than water and its spreading at the interface leads to motion of the gel. The hydrophobic alkyl chains of the gel impart to the surface permselective properties, whereby an organic solvent from inside the gel can be ejected whereas water from outside cannot penetrate the gel. The surface of the gel released the swelling solvent and was rendered crystalline soon after it came into contact with water, while the interior responded more slowly. This process set up an osmotic as well as a hydrostatic pressure across the crystalline, permselective skin that allowed a gradual ejection of the organic solvent and resulted in prolonged motion of the gel (Figure 3). When the asymmetry in solvent release was accentuated by covering all but the rear end of the gel, a more directed and prolonged motion was observed.

The above examples of locomotion rely on some chemical or physical process that affects the surface tension at an interface. In the simplest and most general sense, the velocity, v, of the moving objects can be described as a roughly linear function of the interfacial tension gradient ($\nabla\gamma$), such that $v = k\nabla\gamma$, in which k includes geometric parameters and physical properties such as viscosity. Once set into motion, these moving objects are positioned asymmetrically to one side of the interfacial tension gradients responsible for their motion. Because the objects themselves are also the source of these propulsive gradients, these gradients are continually reestablished as the objects move.

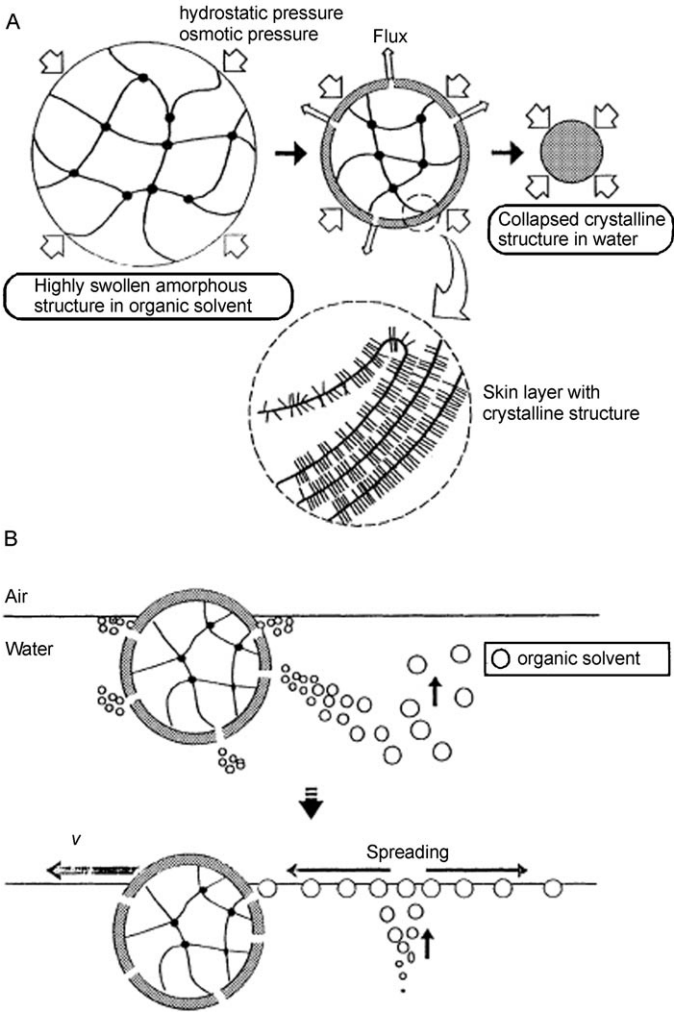

Figure 3. A) Schematic of a solvent-swollen amphiphilic polymer gel. B) The mechanism for its motion due to solvent spreading at the air–water interface. From Ref. [28].

5. Catalytic Systems

Though the synthetic systems described in Section 4 are characterized by simplicity in design, they are all dissipative and hence limited in applicability. Designing application-oriented chemical locomotors requires incorporation of the lessons learned from natural as well as artificial systems, while bearing in mind the limitations presented by the synthetic components used to make them. Many natural systems localize enzymes that act on reagents available in the vicinity, as with the *Listeria* example described in Section 3. From a chemist's perspective, this translates to placement of a catalyst engine on the body of the object where neither engine nor body is consumed when placed in an environment containing the catalyst substrate. The asymmetry in particle design translates into asymmetry in the distribution of reaction products when placed in a suitable "fuel" solution. This use of catalysis and asymmetry would be the most simple and feasible way to power a nanomotor. As discussed in this section, the localized reactions that occur at catalytic sites can

provide motility through a number of mechanisms, including bubble propulsion, diffusiophoresis, interfacial tension gradients, self-electrophoresis, bioelectrochemical propulsion, and cyclic adsorption/desorption.

5.1. Bubble Propulsion

To our knowledge, Whitesides and co-workers were the first to devise an artificial engine based on a catalyst to move an otherwise inanimate object.[29] The key to their design was the asymmetric placement of platinum on millimeter-sized polydimethylsiloxane (PDMS) structures (Figure 4). When

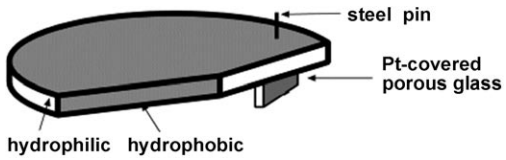

Figure 4. Schematic of a self-propelling object consisting of a PDMS plate (ca. 1–2-mm thick and 9-mm diameter) and a $2\times2\,mm^2$ piece of porous glass filter (covered with platinum by electron beam evaporation) mounted on the PDMS piece with a stainless steel pin. From Ref. [29].

placed in a solution of hydrogen peroxide, the platinum-catalyzed decomposition of hydrogen peroxide to water and oxygen gas led to a jet of bubbles which propelled the objects at the liquid–air interface. This spontaneous motion facilitated the study of self-assembly phenomena by increasing the rate of collisions between objects with both hydrophobic and hydrophilic regions. Close approach of structures resulted in an attractive force arising from the decrease in the total area of the water–air interface, but the force driving the motion of the objects was provided by the catalytic reaction.

Feringa and co-workers described a similar system, which involved the decomposition of hydrogen peroxide by using a manganese-based catalase mimic, rather than platinum, to propel asymmetric silica particles (80-μm diameter).[30] The catalyst was bound to the entire surface of the aminopropyl-modified silica particles by imine linkages. The translational motion of these particles when placed in a solution of hydrogen peroxide was related to the expansion of oxygen bubbles that nucleated on their surface. Although the motor design did not involve localized placement of the catalyst, motility in this case was facilitated by the inhomogeneous distribution of bubble nucleation sites on the asymmetric particle.

5.2. Diffusiophoresis

Besides the generation of bubbles of a gaseous reaction product, such as oxygen, gradients of soluble or nongaseous reaction products themselves are known to induce motion of colloidal particles in solution. In this process of diffusiophoresis, the speed and direction of motion depend on the interaction between the particle surface and the solute, as well as on the magnitude of the solute gradient. A closely related phenomenon is the osmophoresis of a semipermeable vesicle through an osmotic pressure gradient in the surrounding fluid that causes the particle to move to regions of decreasing solute concentration.[31] Both diffusiophoresis and osmophoresis result in fluid transport as a result of concentration gradients of solute and cause motion of particles exposed to such gradients. Although these effects have been described theoretically[6] and demonstrated practically[5] by considering only externally imposed concentration fields, it was proposed by Ajdari and co-workers that this same phenomenon should be observed when the objects themselves are the source of the chemical gradients (Figure 5).[32] This process would occur, for example, if a particle with a catalyst on one side causes an asymmetric distribution of reaction products around the particle.

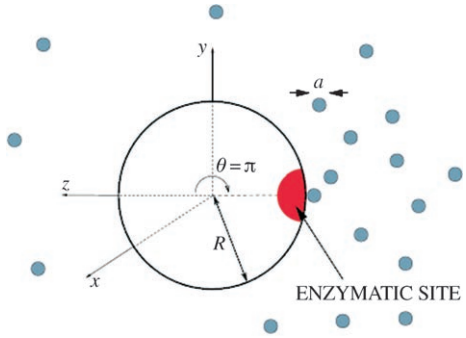

Figure 5. A spherical particle with a spatially defined reaction site. The generation and diffusion of products from this site results in an asymmetric distribution of reaction products around the particle. From Ref. [32].

5.3. Interfacial Tension Gradients

Colloidal particles with catalytic asymmetry can be electrochemically fabricated and indeed exhibit motion when placed in a solution containing a fuel. Prior to the proposal made by Ajdari and co-workers, Paxton et al. reported the autonomous motion of platinum–gold nanorods in aqueous hydrogen peroxide solutions.[33] The rods, with a diameter of 370 nm, consisted of platinum and gold segments, each 1-μm long, and moved at linear speeds of up to 20 $\mu m\,s^{-1}$ (Figure 6). The axial velocity of the rods was related to the rate of the decomposition of hydrogen peroxide, with the rods moving slower in solutions with a lower concentration of hydrogen peroxide. More recently, Fisher et al. have examined the

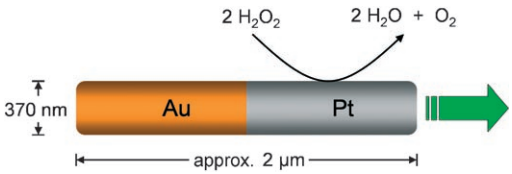

Figure 6. Schematic of an asymmetric Pt–Au nanorod driven by the catalytic decomposition of hydrogen peroxide. From Ref. [33].

motion of these rods at water–organic interfaces to probe the effect of viscosity on rod velocity.[34] Ozin, Manners, and coworkers also reported a similar phenomenon using nickel–gold nanorods, emphasizing the rotational motion imparted to the "nanorotors" induced by the decomposition of hydrogen peroxide.[35]

Rotors of another kind were fabricated lithographically by Catchmark et al.[36] Gold sprockets with a diameter of approximately 150 μm were decorated with platinum on one side of each tooth (Figure 7) to impart catalytic asymmetry to

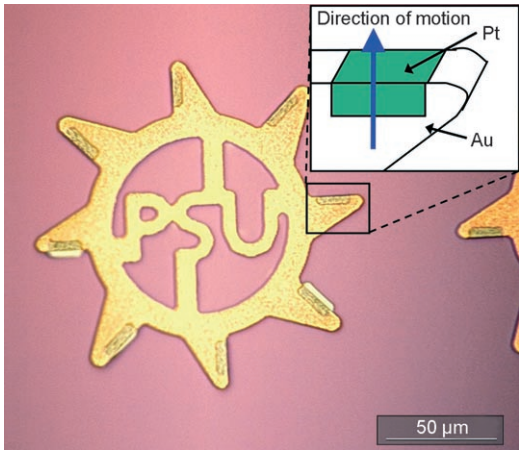

Figure 7. Photograph of a gold gearlike structure with platinum deposited on the tooth regions. The arrow in the inset shows the region where the interfacial tension gradient is formed. From Ref. [39].

the structure and resulted in rotary motion. The linear speed at the circumference of the rotors was 390 $\mu m\,s^{-1}$. Interestingly, the motion of the objects is *towards* the region of high concentration of product (oxygen), rather than away from it, unlike the larger structures described by the groups of Whitesides[29] and Feringa.[30]

In addition to controlling the motion of the systems driven by hydrogen peroxide by geometric design of moving structures, motion may also be controlled magnetically. Kline et al. demonstrated that nanorods, which contain magnetic segments, powered by hydrogen peroxide could be aligned when an external magnetic field is applied.[37] Nickel segments with a length shorter than the segment radius were used to ensure the easy axis of magnetization was orthogonal to the direction of motion (Figure 8). This setup allowed them to show that the motion of the rods was propelled by the decomposition of hydrogen peroxide (and not by attraction to the magnet) and that their direction could be remotely controlled by using relatively weak magnetic fields. This motion is analogous to the behavior of motile bacteria that align themselves with the weak magnetic field of the Earth; in fact, these magnetotactic bacteria have magnetic moments on the same order as that of the nickel-containing rods ($10^{-15}\,A\,m^2$).[38]

Bubbles were generally not observed near the moving objects in any of these examples, demonstrating that bubble propulsion is not responsible for the observed motion and

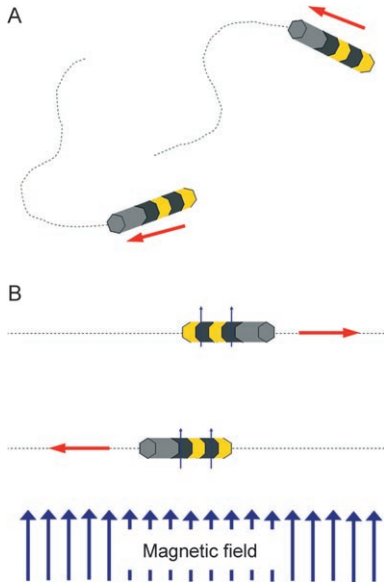

Figure 8. The movement of Pt-Ni-Au-Ni-Au rods in aqueous H_2O_2 without a magnetic field applied (A) and with an applied field (B). Note that rods align perpendicular to the applied magnetic field which results in rod motion about 90 degrees to the applied field. From Ref. [37].

indicating a different propulsion mechanism from that observed by Whitesides[29] and later by Feringa.[30] The motion of these rods was initially attributed to the oxygen concentration gradient emanating from the catalytically active platinum surfaces. Although this process seems a good candidate for a diffusiophoretic mechanism, recent calculations indicated that diffusiophoretic contributions to the motion of these particles would be too small to be the primary driving force and predicted motion in the wrong direction.[39] Instead, it was suggested that the oxygen concentration gradient resulted in an asymmetric interfacial tension gradient around the Pt–Au nanorod that induced a slip velocity at the particle–fluid interface. By solving the convection–diffusion equation to describe the oxygen concentration gradient and by considering the geometric parameters of the nanorods and the surface tension of the bulk solution, the velocity of the Pt–Au nanorods in hydrogen peroxide solutions was reduced to the relationship given in Equation (1), in which S is the surface-normalized oxygen evolu-

$$v \propto \frac{SR^2\gamma}{\eta DL} \qquad (1)$$

tion rate, γ is the surface tension of the bulk solution, D is the rate of diffusion of oxygen away from the rod, and R and L are the geometric radius and length of the nanorods, respectively.

The observed linear relationship between the speed of Pt–Au rods in hydrogen peroxide solutions and the product of the rate of oxygen evolution and surface tension of the bulk solution seemed to confirm this relationship.[33] However, it did not necessarily exclude the possibility of a self-electrophoretic or some other unknown mechanism.

5.4. Self-Electrophoresis

Self-electrophoresis is the migration of a particle in an electric field that is generated by the particle itself, an idea that was first suggested by Mitchell as a mode of transport for microorganisms.[40] Lammert et al. explored the possibility that a cell with an uneven distribution of ion channels on its surface could self-generate an electric field to propel itself through solution.[41] It was shown that the ability of an object to exhibit self-electrophoresis is directly related to its electrophoretic mobility [Eq. (2)]; v is the velocity of the object

$$v = -\mu E_o \tag{2}$$

undergoing self-electrophoresis, μ is the electrophoretic mobility, and E_o is the magnitude of the self-generated electric field parallel to the cell membrane.

This relationship in fact proved to be useful in ruling out self-electrophoresis as a mechanism for the motility of *Synechococcus* cyanobacteria because these marine bacteria failed to exhibit mobility in their natural environment in the presence of an externally applied field.[42] The motility mechanism of these bacteria is still currently under investigation.[43]

Paxton et al. presented a theoretical analysis for a micrometer-sized conducting particle that produces an electric field as a result of redox chemistry occurring at its two ends.[39] One end of the particle carries out oxidation of species A, which sets up an electron flow to the other end of the particle where reduction of species B occurs. Simultaneously, protons are produced at one end and consumed at the other. As these protons migrate, they drag the fluid with them to cause an observable slip velocity, which propels the particle in the opposite direction (Figure 9). It is evident that the speed of

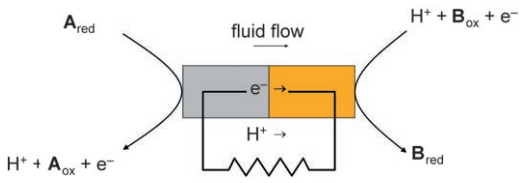

Figure 9. A particle capable of generating its own electric field due to bipolar catalysis. Protons generated when **A** is oxidized on one end migrate along the particle–solution interface and are consumed at the opposite end when **B** is reduced. The ensuing ion flux results in a particle slip velocity relative to the surrounding fluid at the particle–fluid interface. From Ref. [39].

the particle would be dependent not only on the magnitude of the current generated in the particle due to the reaction but also on the conductivity of the surrounding fluid. The Hückel equation was used to demonstrate that an ion current density on the order of 5×10^{-4} mA cm^{-2} would suffice to propel a metallic particle with a zeta potential of -40 mV (conductivity: 10^5 S m^{-1}) at 10 μm s^{-1} in an aqueous medium (conductivity: 10^{-5} S m^{-1}). This current density, J, can be related to the rate of a redox reaction involving n electrons according to the Equation (3), where A is the cross-sectional area of current

$$rate = \frac{JA}{nF} \tag{3}$$

flux and F is Faraday's constant.

5.5. Catalytic Fluid Pumping

An interesting aspect of the work involving hydrogen peroxide and metallic structures relates to immobilization of the catalyst onto a fixed surface. While freely suspended metal nanorods move with respect to the bulk solution, by Galilean invariance an immobilized metal structure in the presence of hydrogen peroxide will induce fluid flows at the interface between the structure and the fluid. Kline et al. demonstrated this fluid-pumping effect on a gold surface patterned with silver—another known catalyst for the decomposition of hydrogen peroxide.[44] When aqueous hydrogen peroxide solution which contained colloidal tracer particles was deposited onto these bimetallic surfaces, the tracers either followed a convection-type fluid flow towards the micrometer-sized silver surface or formed patterns as they were pushed away from the catalyst, depending on the zeta potential of the tracer (Figure 10).

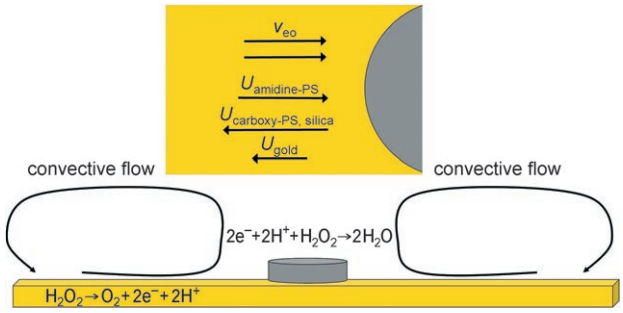

Figure 10. Catalytic fluid pumping on a silver–gold surface. Particles migrate inwards or outwards depending on the zeta potential relative to the zeta potential of the gold substrate. Particles migrating towards the silver catalyst follow electroosmotic convection near the catalyst surface. From Ref. [44].

As in the case of the moving platinum–gold nanorods, the silver catalyst was always in direct electrical contact with the gold. However, when an insulating layer was incorporated between the gold surface and the silver feature, both the convection-driven motion and the pattern formation of the tracers were effectively turned off. The absence of the catalytically driven effect when an insulator separates the two metals is strongly suggestive of an electrokinetic fluid-pumping mechanism resulting from bipolar electrochemistry. It was described that the electric field arises from the silver-catalyzed reduction of hydrogen peroxide and oxidation of hydrogen peroxide on the gold surface, which induces an

electroosmotic flow directed *towards* the silver features. Although particles near the surface–liquid interface are swept inward by this electroosmotic flow, individual particles also experience an electrophoretic force as a result of the catalytically generated electric field, and the direction of this force depends on the zeta potential of the particle. The observed velocity of tracer particles is the sum of the electroosmotic and electrophoretic velocities.

5.6. Bioelectrochemical Propulsion

Bipolar catalysis has also been used to propel the motion of millimeter-scale objects. Mano and Heller described a system based on carbon fibers that exploits two redox-coupled enzymes to induce autonomous motion.[45] An asymmetrically functionalized carbon fiber (0.5–1-cm long; 7-μm wide) was fabricated with one of the ends containing the oxygen-reducing enzyme bilirubin oxidase (BOD) and the other end incorporating glucose oxidase (GOx), which catalyzes the oxidation of glucose to δ-glucono-1,5-lactone. Both enzymes were linked to the carbon fiber using redox polymer bridges to enable efficient electron transport between the enzymes and the conducting fiber (Figure 11). When the fibers were placed at the interface between air and a solution of glucose, they moved in a linear path, with the GOx end forward. This motion was attributed to the difference in surface tension between the two ends caused by the proton flux from anode to cathode. Protons, which are produced in the bipolar oxidation of glucose, are generated at the GOx end and consumed at the BOD end, where cathodic reduction of oxygen takes place to give water. It was proposed that this proton concentration gradient results in surface tension instability and, hence, propulsion of the fiber occurs. To support this hypothesis, they placed an insulating segment between the anode and cathode to prevent the electrochemical reaction and observed no propulsion. Another important observation was that only those fibers at the air–water interface showed mobility. Fibers that were completely immersed in water were immobile, possibly because of the low solubility of oxygen in water.

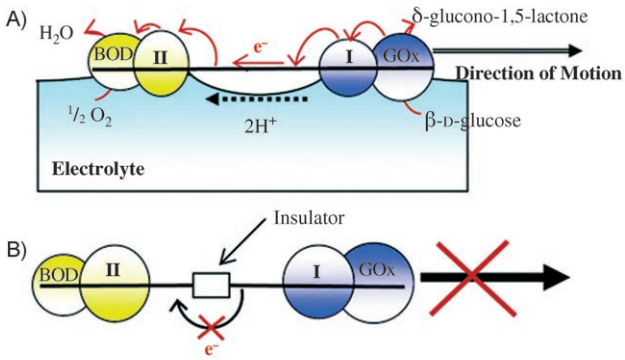

Figure 11. A) A self-propelled bioelectrochemical motor consisting of a carbon fiber functionalized with glucose oxidase (GOx) and redox polymer **I** on one end, and bilirubin oxidase (BOD) and redox polymer **II** on the opposite end. When the fiber is placed on a solution of 10 mM glucose in pH 7 buffer, electrons flow along the path glucose→GOx→**I**→carbon fiber→**II**→BOD→O_2, and the fiber is propelled at the solution–O_2 interface by the ion flow accompanying the flow of electrons. B) The fiber does not move when an insulator is introduced between the two electrocatalytic fiber ends. From Ref. [45].

5.7. Microcantilever-Based Motors

While the examples discussed in this Minireview focus primarily on the motility of unbound objects, transduction of chemical energy to mechanical energy has been achieved in systems such as microcantilevers that are fixed at one end. Microcantilevers find application in the field of sensing, where detection of specific analytes is facilitated by their interaction with a suitably functionalized cantilever.[46] Various modes of signal transduction, such as variations in mass, temperature, and stress, have been employed for sensors based on microcantilever actuation. In the static mode of operation where no driving frequency is applied, the perturbation of the microcantilever due to its interaction with substances in its surroundings is usually detected by means of an optical feedback. Su and Dravid recently described the operation of a catalyst-based cantilever that functions in a cyclic manner.[47] In the presence of UV light, the TiO_2 coated on a cantilever catalyzed the oxidative decomposition of ethanol on its surface, which bent the cantilever as a result of differential stress (Figure 12). Once all the ethanol in the vicinity of the cantilever was consumed by photocatalytic oxidation, the cantilever returned to its original position. The process was repeated when ethanol was reintroduced into the system, allowing the system to function in a cyclic manner, resembling the operation of a combustion engine.

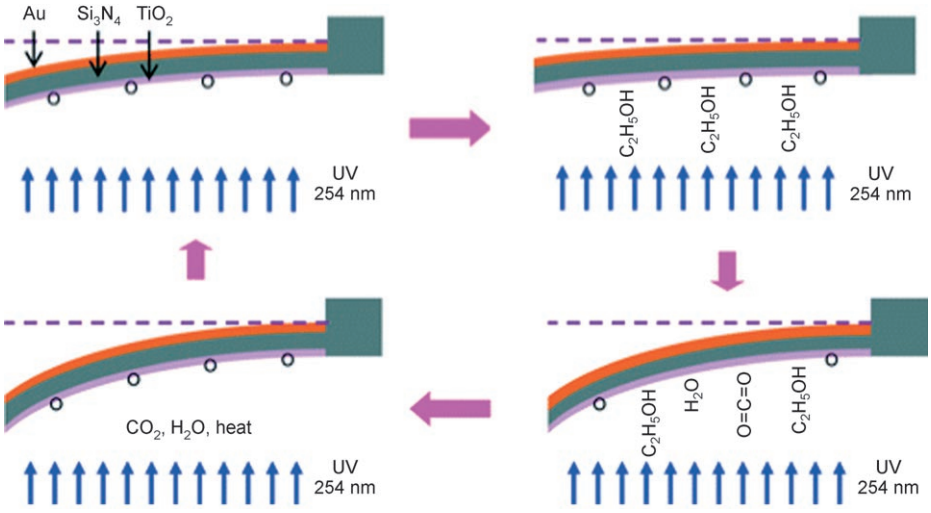

Figure 12. Proposed scheme for ethanol-fuelled photocatalytic microengines based on TiO_2-modified microcantilevers. From Ref. [47].

6. Future Directions and Applications

The small-scale and local conversion of chemical energy into mechanical energy may find use, among other applications, as micropumps and motors for micro- and nanomachinery. As demonstrated by Kline et al., immobilized catalyst systems have the ability to pump fluids without any moving parts.[44] Furthermore, the magnitude of this electrokinetic pumping effect is related to the surface charge on both the moving particles and the substrate in contact with the surrounding fluid. It follows that fluid flow caused by this effect can be modulated by changing the surface charge at solid–fluid interfaces.[48] With appropriate surface chemistry, the properties of the interface may be tuned chemically,[49] electrically,[50] or optically.[51] This catalytically induced electrokinetic phenomenon could find use in microfluidics and lab-on-a-chip applications, where the use of pressure gradients or externally generated electric fields may be difficult or undesirable.

In addition to micropump applications, the ability of particles that are both catalytic and asymmetric to locally convert chemical energy into mechanical energy offers the possibility of designing and controlling micro- and nanoscale machines that can interact with biological systems, such as individual cells. The idea of designing and developing devices that can interact intimately with biological systems at the cellular level is an exciting one and will benefit from addressing two aspects of biocompatibility: one that allows the device to work properly in biological systems, and one that will not interfere in an undesirable way with the biological host. This will require the development of new approaches (or adaptation of current ones) to allow for biocompatible and biologically available materials and fuels.

The examples in this Minireview demonstrate the fulfillment of the minimum requirements for nanoscale machines, namely initiating motion and, to a lesser degree, controlling the direction of that motion at the micro- and nanometer scales. If, in addition to a motor and a director, one could incorporate a device to perform some useful operation such as carrying cargo, entirely new classes of micro- and nanoscale devices may become possible. By incorporating materials that selectively adsorb or desorb a substance upon action of some stimulus from either the immediate environment or a remote source, such devices could be engineered to deliver small-scale amounts of therapeutic agents, or other loads, to specific regions in the human body. In addition, artificial motors could be integrated with biological cells to enhance natural immune responses. For example, synthetic motors attached to leukocytes might increase the rate of movement of these natural defenders especially through capillaries, thus increasing the likelihood that they will find immune-triggering pathogens and may accelerate recovery from or entirely prevent illness.

In charting future directions, two major areas will need to be addressed. First, while we know that catalysts can be used to impart motion to otherwise inanimate objects, we need to more fully understand and develop the mechanisms of chemical-to-mechanical energy transduction. Although some mechanisms of this energy transduction have been discussed here, important work must be done to explore more fully the parameters related to moving small-scale devices, such as the scaling of different mechanisms.

Other mechanisms may also be of interest, such as *Listeria*-mimicking systems propelled by an insertion polymerization mechanism as demonstrated by the motility of ActA-functionalized microspheres in an actin-rich environment.[18] The asymmetric polymerization of monomers at an immobilized metal catalyst will be a biomimetic analogue of the actin-polymerizing *Listeria* system. The ideal system of this type would produce relatively stiff polymer strands at rates equivalent to chains extending by tens of micrometers per second. This corresponds to polymer growth rates on the order of 10^{-5} mol cm^{-2} s^{-1} or site-turnover rates (assuming coverage of about 10^{10} catalyst molecules per cm^2) of approximately 10^5 s^{-1}. The catalyst particle would move by extending a growing polymer chain, akin to the method employed by *Listeria*.[16]

More work must also be done to generalize these phenomena. There are several approaches to convert stored chemical energy into mechanical energy. However, these approaches use a very narrow group of catalytic reactions to convert chemical energy into mechanical energy, which severely limits the usefulness of artificial chemical locomotion at the small scale. Understanding the mechanisms that use asymmetry to induce motion in fluids on the small scale and broadening the class of practical reactions that are capable of utilizing these mechanisms are two key objectives to generalize the phenomena described above. The resulting creative insight and broadened library of reactions will allow tailoring of chemical locomotors to a variety of applications, some of which have been discussed in this Minireview.

We gratefully acknowledge the contributions of our collaborators on this project, in particular Timothy Kline, Jeffrey Catchmark, Paul Lammert, Vincent Crespi, Shyamala Subramanian, Yang Wang, and Darrell Velegol. This work was supported by the Penn State Center for Nanoscale Science, NSF grant DMR-0213623, and NSF-NIRT grant CTS-0506967.

Received: January 6, 2006
Published online: July 31, 2006

[1] M. Shilwa, G. Woehlke, *Nature* **2003**, *422*, 759–765.
[2] *Interfacial Electrokinetics and Electrophoresis* (Ed.: Á. V. Delgado), Marcel Dekker, New York, **2002**.
[3] a) H. Watarai, M. Suwa, Y. Iiguni, *Anal. Bioanal. Chem.* **2004**, *378*, 1693–1699; b) T. M. Vickrey, J. A. Garcia-Ramirez, *Sep. Sci. Technol.* **1980**, *15*, 1297–1304.
[4] a) R. Piazza, *J. Phys.: Condens. Matter* **2004**, *16*, S4195–S4211; b) B. V. Derjaguin, N. V. Churev, V. M. Muller, *Surface Forces* (Engl. transl.), Consultants Bureau, New York, **1987**.
[5] a) H. J. Keh, Y. K. Wei, *Colloid Polym. Sci.* **2000**, *270*, 539–546; b) J. P. Ebel, J. L. Anderson, D. C. Prieve, *Langmuir* **1988**, *4*, 396–406; c) M. M. Lin, D. C. Prieve, *J. Colloid Interface Sci.* **1983**, *95*, 327–339.
[6] J. L. Anderson, *Annu. Rev. Fluid Mech.* **1989**, *21*, 61–99.
[7] a) S. M. Block, *Nature* **1992**, *360*, 493–495; b) A. Ashkin, *IEEE J. Sel. Top. Quantum Electron.* **2000**, *6*, 841–856.

[8] R. Agarwal, K. Ladavac, Y. Roichman, G. Yu, C. M. Lieber, D. G. Grier, *Opt. Express* **2005**, *13*, 8906 – 8912.
[9] F. W. Went, *Am. Sci.* **1968**, *56*, 400 – 413.
[10] E. M. Purcell, *Am. J. Phys.* **1976**, *45*, 3 – 11.
[11] J. Happell, H. Brenner, *Low Reynolds Number Hydrodynamics*, Prentice Hall, Englewood Cliffs, **1965**.
[12] J. Lee, C.-J. Kim, *Proc. IEEE MEMS Workshop* **1998**, 538 – 543.
[13] A. Einstein, *Investigations on the Theory of Brownian Movement*, Dover, New York, **1956**.
[14] J. B. Waterbury, J. M. Willey, D. G. Franks, F. W. Valois, S. W. Watson, *Science* **1985**, *230*, 74 – 76.
[15] J. J. Schmidt, C. D. Montemagno, *Annu. Rev. Mater. Res.* **2004**, *34*, 315 – 337.
[16] D. Pantaloni, C. L. Clainche, M.-F. Carlier, *Science* **2001**, *292*, 1502 – 1506.
[17] A. Upadhyaya, A. van Oudenaarden, *Curr. Biol.* **2003**, *13*, R734 – R744.
[18] L. A. Cameron, M. J. Footer, A. van Oudenaarden, J. A. Theriot, *Proc. Natl. Acad. Sci. USA* **1999**, *96*, 4908 – 4913.
[19] K. J. Bohm, R. Stracke, P. Muhlig, E. Unger, *Nanotechnology* **2001**, *12*, 238 – 244.
[20] L. Jia, S. G. Moorjani, T. N. Jackson, W. O. Hancock, *Biomed. Microdevices* **2004**, *6*, 67 – 74.
[21] M. Platt, G. Muthukrishnan, W. O. Hancock, M. E. Williams, *J. Am. Chem. Soc.* **2005**, *127*, 15686 – 15687.
[22] R. K. Soong, G. D. Bachand, H. P. Neves, A. G. Olkhovets, H. G. Craighead, C. D. Montemagno, *Science* **2000**, *290*, 1555 – 1558.
[23] S. Rozhok, C. K.-F. Shen, P. H. Littler, Z. Fan, C. Liu, C. A. Mirkin, R. C. Holz, *Small* **2005**, *1*, 445 – 451.
[24] D. B. Weibel, P. Garstecki, D. Ryan, W. R. DiLuzio, M. Mayer, J. E. Seto, G. M. Whitesides, *Proc. Natl. Acad. Sci. USA* **2005**, *102*, 11963 – 11967.
[25] A. K. Schmid, N. C. Bartelt, R. Q. Hwang, *Science* **2000**, *290*, 1561 – 1564.
[26] a) N. Watanabe, K. Kutsumi, O. Sano, *J. Phys. Soc. Jpn.* **1994**, *63*, 2955 – 2963; b) O. Sano, K. Kutsumi, N. Watanabe, *J. Phys. Soc. Jpn.* **1995**, *64*, 1993 – 1999.
[27] a) L. Raleigh, *Proc. R. Soc. London* **1890**, *47*, 364; b) S. Nakata, S. Hiromatsu, H. Kitahata, *J. Phys. Chem. B* **2003**, *107*, 10557 – 10559; c) M. I. Kohira, Y. Hayashima, M. Nagayama, S. Nakata, *Langmuir* **2001**, *17*, 7124 – 7129.
[28] T. Mitsumata, J. P. Gong, Y. Osada, *Polym. Adv. Technol.* **2001**, *12*, 136 – 150.
[29] R. F. Ismagilov, A. Schwartz, N. Bowden, G. M. Whitesides, *Angew. Chem.* **2002**, *114*, 674 – 676; *Angew. Chem. Int. Ed.* **2002**, *41*, 652 – 654.
[30] J. Vicario, R. Eelkema, W. R. Browne, A. Meetsma, R. M. La Crois, B. L. Feringa, *Chem. Commun.* **2005**, 3936 – 3938.
[31] J. L. Anderson, *Phys. Fluids* **1983**, *26*, 2871 – 2879.
[32] R. Golestanian, T. B. Liverpool, A. Ajdari, *Phys. Rev. Lett.* **2005**, *94*, 220801 – 220804.
[33] W. F. Paxton, K. C. Kistler, C. C. Olmeda, A. Sen, S. K. St. Angelo, Y. Cao, T. E. Mallouk, P. E. Lammert, V. H. Crespi, *J. Am. Chem. Soc.* **2004**, *126*, 13424 – 13431.
[34] P. Dhar, T. M. Fischer, Y. Wang, T. E. Mallouk, W. F. Paxton, A. Sen, *Nano Lett.* **2006**, *6*, 66 – 72.
[35] a) S. Fournier-Bidoz, A. C. Arsenault, I. Manners, G. A. Ozin, *Chem. Commun.* **2005**, 441 – 443; b) Review: G. A. Ozin, I. Manners, S. Fournier-Bidoz, A. Arsenault, *Adv. Mater.* **2005**, *17*, 3011 – 3018.
[36] J. M. Catchmark, S. Subramanian, A. Sen, *Small* **2005**, *1*, 202 – 206.
[37] T. R. Kline, W. F. Paxton, T. E. Mallouk, A. Sen, *Angew. Chem.* **2005**, *117*, 754 – 756; *Angew. Chem. Int. Ed.* **2005**, *44*, 744 – 746.
[38] H. Lee, A. M. Purdon, V. Chu, R. M. Westervelt, *Nano Lett.* **2004**, *4*, 995 – 998.
[39] W. F. Paxton, A. Sen, T. E. Mallouk, *Chem. Eur. J.* **2005**, *11*, 6462 – 6470.
[40] P. Mitchell, *FEBS Lett.* **1972**, *28*, 1 – 4.
[41] P. E. Lammert, J. Prost, R. Bruinsma, *J. Theor. Biol.* **1996**, *178*, 387 – 391.
[42] T. P. Pitta, H. C. Berg, *J. Bacteriol.* **1995**, *177*, 5701 – 5703.
[43] B. Brahamsha, *J. Mol. Microbiol. Biotechnol.* **1999**, *1*, 59 – 62.
[44] T. R. Kline, W. F. Paxton, Y. Wang, D. Velegol, T. E. Mallouk, A. Sen, *J. Am. Chem. Soc.* **2005**, *127*, 17150 – 17151.
[45] N. Mano, A. Heller, *J. Am. Chem. Soc.* **2005**, *127*, 11574 – 11575.
[46] a) *Encyclopedia of Nanoscience and Nanotechnology*, *Vol. 1* (Ed.: H. S. Nalwa), American Scientific, Stevenson Ranch, **2004**, pp. 499 – 516; b) R. Raiteri, M. Grattarola, H.-J. Butt, P. Skladal, *Sens. Actuators B* **2001**, *79*, 115 – 126.
[47] M. Su, V. P. Dravid, *Nano Lett.* **2005**, *5*, 2023 – 2028.
[48] T. M. Squires, M. Z. Bazant, *J. Fluid Mech.* **2004**, *509*, 217 – 252.
[49] X. Zhang, R. Bai, *Langmuir* **2003**, *19*, 10703 – 10709.
[50] J. Lahann, S. Mitragotri, T. Tran, H. Kaido, J. Sundaran, S. Hoffer, G. A. Somorjai, R. Langer, *Science* **2003**, *299*, 371 – 374.
[51] D. G. Walter, D. J. Campbell, C. A. Mirkin, *J. Phys. Chem. B* **1999**, *103*, 402 – 405.